

Model of Fabry-Pérot-type electromagnetic modes of a cylindrical nanowire

V. G. Bordo*

NanoSyd, Mads Clausen Institute, Syddansk Universitet, Alsion 2, DK-6400 Sønderborg, Denmark

(Received 19 November 2009; revised manuscript received 23 December 2009; published 21 January 2010)

The rigorous theory of normal electromagnetic modes of a cylindrical nanowire of finite length is developed. The exact integral equation which determines the solution of Maxwell's equations obeying the boundary conditions at the whole nanowire surface is derived. The nanowire normal (Fabry-Pérot) modes are defined as nontrivial solutions of the source-free equation. The approach is considered in more detail for elongated nanowires whose length is much larger than their diameter. The resonance condition obtained for a single-mode nanowire resembles the formula for the Fabry-Pérot resonator if one introduces an effective wavelength-dependent phase shift which can be determined from the calculation of the nanowire response function.

DOI: [10.1103/PhysRevB.81.035420](https://doi.org/10.1103/PhysRevB.81.035420)

PACS number(s): 41.20.Jb, 42.25.Fx, 78.67.Lt, 81.07.-b

I. INTRODUCTION

Recently, nanowires (NWs), both semiconductor and metallic, have attracted growing attention due to their significant potential for applications in future nanodevices. Semiconductor NWs demonstrate remarkable photoluminescence, waveguiding and lasing properties that makes them very promising as active elements in optics and optoelectronics on a nanoscale.¹⁻³ On the other hand, metallic NWs support surface-plasmon polaritons which are able to squeeze light into nanometer dimensions, producing large local-field enhancement, that can find diverse applications in nanoplasmonics.^{4,5} Besides that, NWs can act as a nanoantenna which concentrates radiation from a distant source or, vice versa emits efficiently a localized field into the outer space.⁶⁻⁸

Being an optical resonator, a NW enhances electromagnetic waves of certain frequencies which are determined by the resonator length and which are known as Fabry-Pérot modes. They can be observed as distinct peaks in NW photoluminescence or light-scattering spectra.⁹⁻¹⁴ Under pumping conditions above threshold, those peaks evolve into the lasing spectrum.¹⁵⁻¹⁷ Thus a knowledge of Fabry-Pérot modes is of considerable importance for the development of a nanowire laser or, in the case of metallic NWs, a spaser which generates coherent surface plasmons.¹⁸ Moreover, a proper determination of Fabry-Pérot modes is crucial for the reconstruction of the dispersion curves of the NW waveguide modes.¹⁹

The concept of Fabry-Pérot modes dates back to classical optics and originates from interference between multiple reflections of light propagating between two parallel semitransparent plates.²⁰ The condition of constructive interference between the light beams traveling in one direction gives the wavelengths for which the transmission through the two plates is maximum. This consideration assumes that the light beam is not confined in the transverse direction by a boundary surface and its diameter is much larger than its wavelength. This is obviously not the case for a nanowire and the whole concept must be revised from the beginning.

The lack of a rigorous theory enforces one to use the approaches beyond their applicability. One frequently considers the confinement of the electromagnetic field in a nano-

wire waveguide and reflections at the nanowire ends as two completely independent problems.⁸ By this means, one obtains the ordinary waveguide modes of an infinite cylinder for the waves propagating along the nanowire which are enhanced at the wavelengths corresponding to classical Fabry-Pérot modes. As a result, it is expected that the intermode spacing is proportional to the inverse nanowire length and only slightly varies due to the nanowire refractive index dispersion. More systematic studies reveal, however, some discrepancies between the positions of the observed peaks and the calculated Fabry-Pérot modes.^{9-12,21-24} Let us note that this problem is not specific for cylindrical symmetry of a nanoresonator and occurs also for metal strips, as an example.^{25,26}

The paper is organized as follows. In Sec. II we present a general approach to the problem which is then considered in the limit of elongated nanowires. The particular case of a single-mode nanowire is discussed as well. Sec. III gives numerical examples calculated for a single-mode nanowire along with their discussion. The main results are summarized in Sec. IV.

II. THEORETICAL MODEL

A. General approach

Let a nanowire has the shape of a circular cylinder with the radius a and the length L . Let its optical properties be described by the dielectric function ϵ_2 and it is surrounded by medium with the dielectric function ϵ_1 . A source-free solution of Maxwell's equations can be found in terms of the electric and magnetic Hertz vectors, $\mathbf{\Pi}^e$ and $\mathbf{\Pi}^m$, respectively.²⁷ Assuming the temporal dependence of the fields in the form of $\exp(-i\omega t)$, one can obtain the electric and magnetic field amplitudes in Gaussian units as follows:

$$\mathbf{E}_j = \nabla(\nabla \cdot \mathbf{\Pi}_j^e) + k_j^2 \mathbf{\Pi}_j^e + i \frac{\omega}{c} \nabla \times \mathbf{\Pi}_j^m, \quad (1)$$

$$\mathbf{H}_j = \nabla(\nabla \cdot \mathbf{\Pi}_j^m) + k_j^2 \mathbf{\Pi}_j^m - i \epsilon_j \frac{\omega}{c} \nabla \times \mathbf{\Pi}_j^e, \quad (2)$$

where ω is the field frequency, c is the speed of light in vacuum, $k_j = (\omega/c) \sqrt{\epsilon_j} = (2\pi/\lambda) \sqrt{\epsilon_j}$ with λ the wavelength in

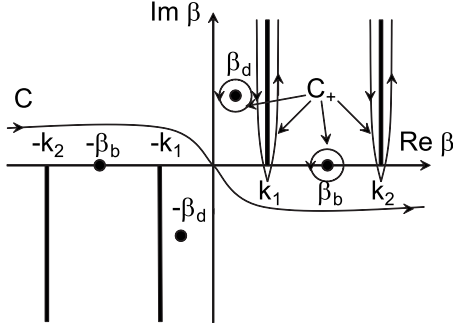


FIG. 1. Complex plane of β with the cuts, poles and integration paths. For simplicity, only a single waveguide mode (β_b) and a single decaying mode (β_d) are indicated. The integration path C_+ includes also the arcs of an infinite radius which are not shown.

vacuum and the subscript j labels the quantities outside the nanowire ($j=1$) or inside it ($j=2$). A rigorous solution of the problem under consideration can be constructed in two steps. First, we shall introduce a solution of Maxwell's equations which satisfies the necessary boundary conditions at the nanowire ends. Second, we shall use this auxiliary solution to find a solution for which the tangential field components are continuous across all the boundaries. Let the origin of the cylindrical coordinate system $\mathbf{R}=(r, \theta, z)$ be located at the nanowire center and its z axis is directed along the nanowire axis. We shall seek the z component of the solution in the interval $-L/2 < z < L/2$ as a superposition of the z components of the electric and magnetic Hertz vectors, Ψ_j^e and Ψ_j^m , respectively. The latter quantities can be represented as the Fourier integrals

$$\Psi_j^\sigma(r, \theta, z) = \frac{1}{2\pi} \int_C \tilde{\Psi}_j^\sigma(r, \theta; \beta) e^{i\beta z} d\beta, \quad (3)$$

where the integration path C lies in the complex plane of propagation constants β to ensure the generality of the solution and the superscript $\sigma=e, m$ labels the type of the field component. The Fourier transforms $\tilde{\Psi}_j^\sigma$ in their turn can be expanded in the elementary waves of a cylinder

$$\tilde{\Psi}_j^\sigma(r, \theta; \beta) = \frac{1}{q_j} \sum_{n=-\infty}^{\infty} a_{jn}^\sigma(\beta) Z_n(q_j r) e^{-in\theta}, \quad (4)$$

where $Z_n(\rho)$ is a cylindrical function defined as

$$Z_n(q_j r) = \begin{cases} J_n(q_2 r) & \text{if } r < a; \\ H_n^{(1)}(q_1 r) & \text{if } r > a, \end{cases} \quad (5)$$

with J_n and $H_n^{(1)}$ the Bessel function and the Hankel function, respectively, n is an integer and $q_j = \sqrt{k_j^2 - \beta^2}$. The branch points $\beta = \pm k_j$ specify the cuts on the complex plane of β which are shown in Fig. 1 along with the integration path C . The Hertz vectors [Eq. (3)] provide a solution of Maxwell's equations by the construction. Let us postulate now a zero electromagnetic field in the regions $z < -L/2$ and $z > L/2$. Then there will be jumps in the tangential field components across the planes $z = -L/2$ and $z = L/2$. According to the Schelkunoff's formulation of the equivalence theorem,²⁸ the

fields originating from the reflection at the nanowire ends can be found as they would be induced by the fictitious surface electric and magnetic current sheets with the surface densities

$$\mathbf{K}_{j\pm}^e = \pm \frac{c}{4\pi} \mathbf{e}_z \times \mathbf{H}_{j\pm,t}, \quad \mathbf{K}_{j\pm}^m = \mp \frac{c}{4\pi} \mathbf{e}_z \times \mathbf{E}_{j\pm,t}, \quad (6)$$

respectively, where \mathbf{e}_z is the unit vector along the z axis, the subscript t denotes the components which are tangential to the facets and $-$ and $+$ subscripts correspond to the nanowire facets at $z = -L/2$ and $z = L/2$, respectively. Here the quantities $\mathbf{H}_{j\pm,t}$ and $\mathbf{E}_{j\pm,t}$ can be expressed in terms of the coefficients a_{jn}^σ using Eqs. (1)–(5) taken at $z = \pm L/2$. The Hertz vectors of the fields originating from the fictitious currents are the solutions of inhomogeneous wave equations with the sources given by Eq. (6) and are found as

$$\Phi_{j\pm}^\sigma(\mathbf{R}) = \frac{i}{\tau_j^\sigma \omega} \int_{S_{j\pm}} \mathbf{K}_{j\pm}^\sigma(\mathbf{R}') \frac{e^{ik_j |\mathbf{R}-\mathbf{R}'|}}{|\mathbf{R}-\mathbf{R}'|} d\mathbf{R}', \quad (7)$$

where $\tau_j^e = \epsilon_j$, $\tau_j^m = 1$. It is assumed here that the currents $\mathbf{K}_{j\pm}^\sigma$ are taken in the rectangular coordinates (x, y, z) and the radius vector \mathbf{R}' runs over the surfaces $S_{j\pm}$ in the planes $z' = \pm L/2$ with $r' > a$ for $S_{1\pm}$ and $r' < a$ for $S_{2\pm}$. Let us note that the vectors $\Phi_{j\pm}^\sigma$ have only nonzero components perpendicular to the z axis.

Now the solution of Maxwell's equations in the region $-L/2 < z < L/2$ which satisfies the boundary conditions at the NW ends is given by the Hertz vectors

$$\mathbf{\Pi}_j^\sigma = \Phi_{j-}^\sigma + \Phi_{j+}^\sigma + \Psi_j^\sigma \mathbf{e}_z \quad (8)$$

with the coefficients $a_{jn}^\sigma(\beta)$ which are not yet defined. To complete the solution of the problem we shall require that the field components which are tangential to the cylinder surface would be continuous at $r = a$. The result can be written in the form of the matrix homogeneous Fredholm integral equation of the second kind

$$\hat{M}_n(\beta) \vec{A}_n(\beta) = \frac{1}{2\pi} \int_C [e^{-i(\beta-\beta')L/2} - e^{i(\beta-\beta')L/2}] \times \hat{N}_n(\beta, \beta') \vec{A}_n(\beta') d\beta', \quad (9)$$

where $\vec{A}_n(\beta)$ is the column vector

$$\vec{A}_n(\beta) = \begin{pmatrix} a_{2n}^e(\beta) \\ a_{2n}^m(\beta) \\ a_{1n}^e(\beta) \\ a_{1n}^m(\beta) \end{pmatrix}. \quad (10)$$

The explicit form of the matrices \hat{M}_n and \hat{N}_n can be found using the results of Ref. 29 and is given in the Appendix. The condition that this equation has nontrivial solutions determines possible normal modes of a nanowire. The right-hand side of Eq. (9) describes the influence of the nanowire facets. When $L \rightarrow \infty$, due to the rapid oscillations of the integrand, it can be neglected and that condition is reduced to the equation $\det \hat{M}_n(\beta) = 0$ which dictates the normal modes of an infinitely long cylinder. It is worthwhile to note that Eq. (9)

takes a dimensionless form when being written in terms of the dimensionless parameters $\bar{\lambda}=\lambda/a$, $\bar{\beta}=\beta a$ and $\bar{L}=L/a$ that suggests the principle of similitude of different nanowires.³⁰

B. Limit of elongated nanowire

Equation (9) is exact and valid for an arbitrary ratio between the nanowire length, its diameter and the wavelength. It can be investigated numerically using standard methods of the theory of integral equations.³¹ In the present paper, we consider in more detail the case when $L \gg 2a$.

Let us note that the zeros of $\det \hat{M}_n(\beta)$ specify the poles of the amplitudes $\vec{A}_n(\beta)$ in Eq. (9). One can rewrite this equation in the following form:

$$\hat{M}_n(\beta)\vec{A}_n(\beta) = \frac{1}{2\pi} \left[\int_{C_+} e^{-i(\beta-\beta')L/2} \hat{N}_n(\beta, \beta') \vec{A}_n(\beta') d\beta' - \int_{C_-} e^{i(\beta-\beta')L/2} \hat{N}_n(\beta, \beta') \vec{A}_n(\beta') d\beta' \right], \quad (11)$$

where the integration path C_+ runs in the upper half-plane embracing the cuts and the poles in the right half-plane of the complex plane of β (see Fig. 1) while the integration path C_- runs similarly in the lower half-plane embracing the cuts and the poles in the left half-plane (not shown). The contributions from the cut edges can be estimated as being of the order of $(2a/L)^2$ and can be neglected. The remaining integrals are determined by the sum of residuals of the integrands at the poles given by the normal modes of an infinite nanowire, β_a . We shall assume further that the propagation lengths of all transient modes for which β_a is a complex quantity are much less than L . Then the dominant contribution to the integral is given by the waveguide (bound) modes for which β_a are purely real. This approximation leads to the following equation:

$$\hat{M}_n(\beta)\vec{A}_n(\beta) = i \left\{ \sum_b e^{-i(\beta-\beta_b)L/2} \hat{N}_n(\beta, \beta_b) \text{Res}[\vec{A}_n(\beta_b)] + \sum_b e^{i(\beta+\beta_b)L/2} \hat{N}_n(\beta, -\beta_b) \text{Res}[\vec{A}_n(-\beta_b)] \right\}, \quad (12)$$

where $\text{Res}[\vec{A}_n(\beta_b)]$ is a column composed of the residuals of the vector $\vec{A}_n(\beta)$ components at the pole $\beta=\beta_b$. Using the Cauchy's integral formula one can show that

$$\text{Res}[\vec{A}_n(-\beta_b)] = -\text{Res}[\hat{T}\vec{A}_n(\beta_b)] = -\hat{T}\text{Res}[\vec{A}_n(\beta_b)], \quad (13)$$

where \hat{T} is the operator of inversion in the β plane so that

$$\hat{T}\vec{A}_n(\beta) = \vec{A}_n(-\beta). \quad (14)$$

Due to the symmetry of the problem with respect to the reflection in the plane $z=0$ the field amplitudes can be chosen either even or odd relatively the inversion of the z coordinate. The analysis of the Maxwell equations written in the

cylindrical coordinates reveals that the components E_z , H_r , and H_θ have the same parity with respect to the inversion of z whereas the components E_r , E_θ , and H_z have the same opposite parity. This condition is satisfied if the amplitudes a_{jn}^e and a_{jn}^m in Eq. (4) have different parity with respect to the replacement $\beta \rightarrow -\beta$. Taking into account that the quantities a_{jn}^e and a_{jn}^m determine the z components of the electric and magnetic fields, respectively, which are continuous at the nanowire surface $r=a$ we conclude that the pairs of amplitudes a_{1n}^e and a_{2n}^e as well as a_{1n}^m and a_{2n}^m have common parity relatively the inversion of β . In what follows, we shall call the electromagnetic field even or odd if its E_z component is an even or odd function of z , respectively. According to this definition, an even electromagnetic field corresponds to even coefficients a_{1n}^e and a_{2n}^e and odd coefficients a_{1n}^m and a_{2n}^m , whereas for an odd electromagnetic field the parity of the coefficients is opposite. This property determines the explicit form of the operator \hat{T} . For even fields

$$\hat{T}_{even} = \begin{pmatrix} 1 & 0 & 0 & 0 \\ 0 & -1 & 0 & 0 \\ 0 & 0 & 1 & 0 \\ 0 & 0 & 0 & -1 \end{pmatrix}, \quad (15)$$

while for odd fields

$$\hat{T}_{odd} = -\hat{T}_{even}. \quad (16)$$

Now introducing the substitution

$$\vec{A}_n(\beta) = \hat{M}_n^{-1}(\beta)\vec{C}_n(\beta) \quad (17)$$

and taking into account relation (13) one can rewrite Eq. (12) as follows:

$$\vec{C}_n(\beta) = i \left\{ \sum_b e^{-i(\beta-\beta_b)L/2} \hat{N}_n(\beta, \beta_b) - \sum_b e^{i(\beta+\beta_b)L/2} \times \hat{N}_n(\beta, -\beta_b) \hat{T} \right\} \text{Res}[\hat{M}_n^{-1}(\beta_b)]\vec{C}_n(\beta_b), \quad (18)$$

where $\text{Res}[\hat{M}_n^{-1}(\beta_b)]$ is a matrix composed of the residuals of the matrix elements $[\hat{M}_n^{-1}(\beta)]_{kl}$ at the pole $\beta=\beta_b$. The above equation allows one to find the vectors $\vec{C}_n(\beta)$ in terms of the quantities $\vec{C}_n(\beta_b)$ which in their turn satisfy the following set of equations:

$$\vec{C}_n(\beta_a) = i \left\{ \sum_b e^{-i(\beta_a-\beta_b)L/2} \hat{N}_n(\beta_a, \beta_b) - \sum_b e^{i(\beta_a+\beta_b)L/2} \times \hat{N}_n(\beta_a, -\beta_b) \hat{T} \right\} \text{Res}[\hat{M}_n^{-1}(\beta_b)]\vec{C}_n(\beta_b), \quad (19)$$

whose dimension is determined by the number of waveguide modes which are supported by an infinite nanowire of the same radius at a given frequency ω for a given parameter n . Thus the condition that the determinant of Eq. (19) is equal to zero specifies the Fabry-Pérot modes of the nanowire.

The spatial distribution of the electromagnetic field corresponding to the Fabry-Pérot modes can be found using Eq. (18). For this purpose, let us introduce the partial four-component Hertz vector amplitudes as follows:

$$\tilde{\Psi}_n(r, \theta, z) = \frac{1}{2\pi} \int_C \tilde{\tilde{\Psi}}_n(r, \theta; \beta) e^{i\beta z} d\beta, \quad (20)$$

where the Fourier transform $\tilde{\tilde{\Psi}}_n$ is given by

$$\tilde{\tilde{\Psi}}_n(r, \theta; \beta) = e^{-in\theta} \hat{X}_n(r; \beta) \tilde{A}_n(\beta) \quad (21)$$

with

$$\hat{X}_n(r) = \begin{pmatrix} J_n(q_2 r)/q_2^2 & 0 & 0 & 0 \\ 0 & J_n(q_2 r)/q_2^2 & 0 & 0 \\ 0 & 0 & H_n^{(1)}(q_1 r)/q_1^2 & 0 \\ 0 & 0 & 0 & H_n^{(1)}(q_1 r)/q_1^2 \end{pmatrix}. \quad (22)$$

Now taking into account Eqs. (17) and (18) and reducing the integral over the contour C to the sum of the residuals as before one comes to the following equation:

$$\begin{aligned} \tilde{\Psi}_n(r, \theta, z) &= 2e^{-in\theta} \sum_{a,b} e^{i(\beta_b - \beta_a)L/2} \hat{X}_n(r; \beta_a) \hat{S}_a(z) \\ &\quad \times \text{Res}[\hat{M}_n^{-1}(\beta_a)] \hat{N}_n(\beta_a, \beta_b) \text{Res}[\hat{M}_n^{-1}(\beta_b)] \tilde{C}_n(\beta_b), \end{aligned} \quad (23)$$

where \hat{S}_a is a diagonal matrix such that for even modes $S_{a,11} = S_{a,33} = \cos(\beta_a z)$ and $S_{a,22} = S_{a,44} = i \sin(\beta_a z)$, while for odd modes $S_{a,11} = S_{a,33} = i \sin(\beta_a z)$ and $S_{a,22} = S_{a,44} = \cos(\beta_a z)$. Here we have used the identity

$$\hat{M}_n^{-1}(-\beta) \hat{N}_n(-\beta, -\beta') \hat{T} = -\hat{T} \hat{M}_n^{-1}(\beta) \hat{N}_n(\beta, \beta') \quad (24)$$

and we have assumed that the field is calculated at the points which are not too close to the nanowire ends so that $L/2 \pm z \gg a$.

C. Single-mode nanowire

Equation (19) which determines the NW normal modes is written in terms of the propagation constants of an infinitely long nanowire of the same radius as the considered one. We shall define therefore a single-mode regime in the same way as for an infinite nanowire. For dielectric or semiconductor NWs such conditions are realized when the criterion

$$2\pi \frac{a}{\lambda} \sqrt{\epsilon_2 - \epsilon_1} < 2.405 \quad (25)$$

is fulfilled.³² For a single-mode NW which supports only the fundamental waveguide mode HE_{11} ($n=1$) with the propagation constant β_0 Eq. (19) is reduced to a set of four equations. Its normal modes are determined by the roots of the determinant of the matrix

$$\begin{aligned} \hat{O}(\beta_0, L) &= i[\hat{N}_1(\beta_0, \beta_0) - e^{i\beta_0 L} \hat{N}_1(\beta_0, -\beta_0) \hat{T}] \text{Res}[\hat{M}_1^{-1}(\beta_0)] \\ &\quad - \hat{I}, \end{aligned} \quad (26)$$

where \hat{I} is a 4×4 unit matrix. One can see from here that for a given β_0 the matrix $\hat{O}(\beta_0, L)$ is periodic in L : it is not changed on the transformation $L \rightarrow L + (2\pi m / \beta_0)$ with m an integer. On the other hand, it is transformed to the matrix corresponding to the opposite parity if L takes a shift by $\pi m / \beta_0$ [see Eq. (16)]. Therefore the nanowire possesses a sequence of normal modes of alternating parity which obeys the equation

$$\beta_0 L = m\pi - \phi(\beta_0), \quad (27)$$

where $-\pi/2 < \phi(\beta_0) \leq \pi/2$. Here the integer m takes the values $1, 2, 3, \dots$ if $\phi(\beta_0) \geq 0$, while in the range of β_0 where $\phi(\beta_0) < 0$ the zeroth-order mode ($m=0$) can also exist. One has to keep in mind, however, that result (27) has been obtained in the limit of large parameter L/a . Under this assumption such a lowest-order resonance can occur only when $\beta_0 a \ll 1$.

Let us note that Eq. (27) resembles the condition of constructive interference for classical Fabry-Pérot interferometer with the wave vector and the phase shift acquired on reflection being replaced by β_0 and $\phi(\beta_0)$, respectively.²⁰ However this is only formal similarity since for a boundary between two nonabsorbing dielectrics ϕ equals either 0 or π . Moreover, in the case of reflection of a waveguide mode one cannot define the reflection coefficient, and consequently the reflection phase, by analogy with the Fresnel formulas as the ratio of reflected to incident wave amplitude since this quantity depends on the coordinate r .³³ Instead, the function $\phi(\beta_0)$ can be said to be an effective phase shift on reflection.

When a nanowire is excited by an external electromagnetic field of the frequency ω , the roots of $\det \hat{O}(\beta_0, L)$ determine either the values of the propagation constant at a fixed NW length, $\beta_0(L)$, or the values of the NW length at a fixed propagation constant, $L(\beta_0)$, at which the nanowire optical response will be maximum. We shall define therefore the response function as

$$F(\beta_0, L) = |\det \hat{O}(\beta_0, L)|^{-1}. \quad (28)$$

The peaks of $F(\beta_0, L)$ can be identified as originating from Fabry-Pérot modes of a nanowire. The corresponding frequency at which such a resonance will occur is determined by the dispersion relation for the waveguide mode, $\omega(\beta_0)$.

The spatial distribution of the electromagnetic field [Eq. (23)] is reduced in this case to the following one:

$$\begin{aligned} \tilde{\Psi}_1(r, \theta, z) &= 2e^{-i\theta} \hat{X}_1(r; \beta_0) \hat{S}_0(z) \text{Res}[\hat{M}_1^{-1}(\beta_0)] \hat{N}_1(\beta_0, \beta_0) \\ &\quad \times \text{Res}[\hat{M}_1^{-1}(\beta_0)] \tilde{C}_1(\beta_0). \end{aligned} \quad (29)$$

In particular, it follows from here that the z dependence of the Fabry-Pérot mode field component E_z is given by $\cos(\beta_0 z)$ for even modes and by $\sin(\beta_0 z)$ for odd modes. In such a case the order of the mode, m , equals the number of half periods in the field amplitude variation along the nanowire length.

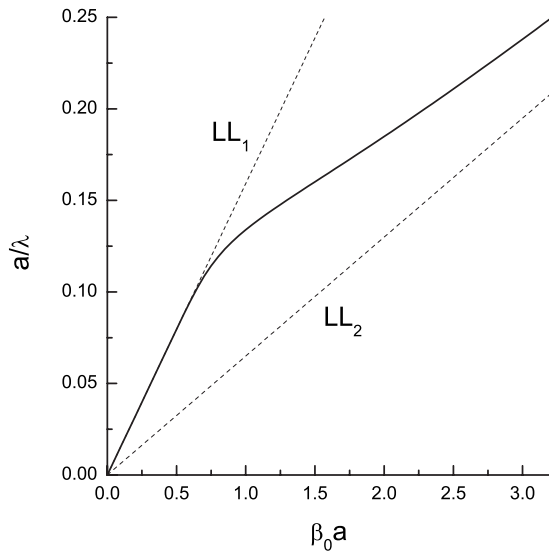


FIG. 2. The dispersion curve of the fundamental waveguide mode HE_{11} for $\epsilon_1=1$ and $\epsilon_2=6$. The straight dash lines LL_1 and LL_2 correspond to the dispersion of light in media with the dielectric functions ϵ_1 and ϵ_2 , respectively.

III. NUMERICAL RESULTS AND DISCUSSION

To illustrate the general theory developed above we shall calculate the Fabry-Pérot resonances for the case when $\epsilon_1=1$ and $\epsilon_2=6$. We shall consider the range of parameters where such a nanowire supports the only waveguide mode with $n=1$, the fundamental mode HE_{11} . According to Eq. (25) this regime takes place when $a/\lambda < 0.171$. However as the NW modes with different indices n are not mixed with each other, the results of Sec. II C are valid in a wider range $a/\lambda < 0.272$ which is below the cutoff for the modes EH_{11} and HE_{12} .³⁴ The dispersion curve of the fundamental mode in this range plotted in the dimensionless parameters $\bar{\beta}_0$ and $\bar{\lambda}$ is given in Fig. 2. The density plots of the response func-

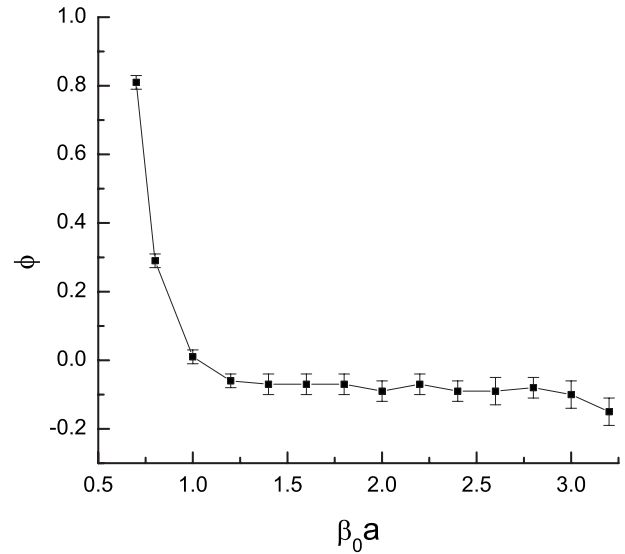


FIG. 4. The parameter ϕ entering into Eq. (27) as a function of the dimensionless propagation constant. The error bars originate from the linear fitting of Eq. (27).

tion in the coordinates $\beta_0-\bar{L}$ calculated for even and odd Fabry-Pérot modes are shown in Figs. 3(a) and 3(b), respectively. The brighter regions in the figures correspond to higher peak intensities. The smeared region at $\beta_0 a < 0.8$ corresponds to the range of the dispersion curve which only slightly differs from the dispersion of light in surrounding medium (see Fig. 2). Due to a low effective refractive index contrast, the reflectivity in this region is small³⁴ and the Fabry-Pérot modes are not well pronounced.

The sequence of the resonance plots represented in Fig. 3 can be characterized by their sections by the planes $\bar{\beta}_0 = \text{constant}$. The positions of the resonances can be fitted very well by formula (27) and from this fitting one can find the quantity $\phi(\beta_0)$ which is plotted in Fig. 4. On the other hand,

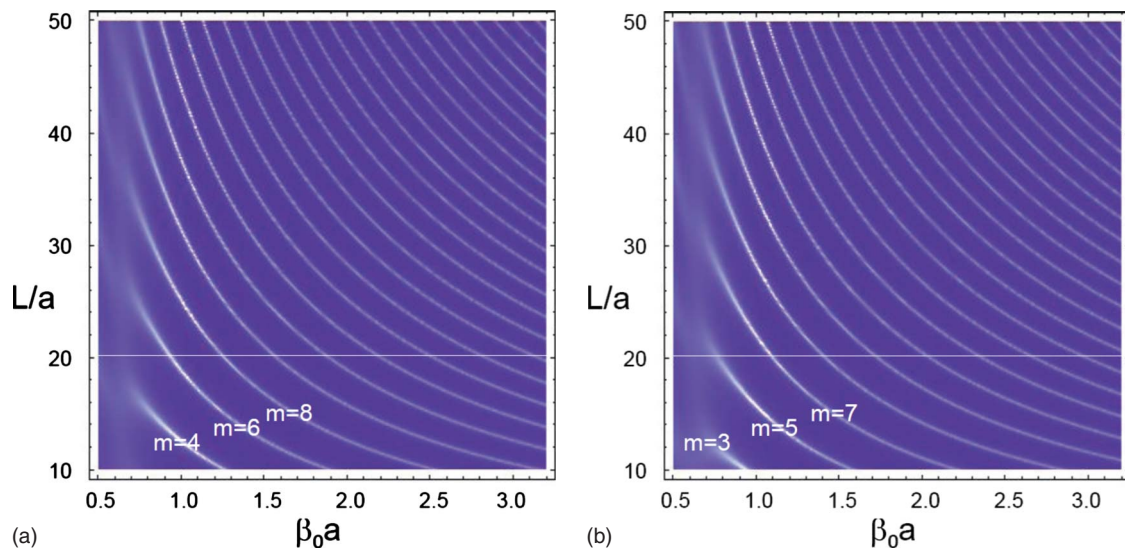


FIG. 3. (Color online) The response function plotted versus the dimensionless propagation constant and NW length for $\epsilon_1=1$ and $\epsilon_2=6$: (a) even modes; (b) odd modes. The orders of the first three resonances in this range are indicated.

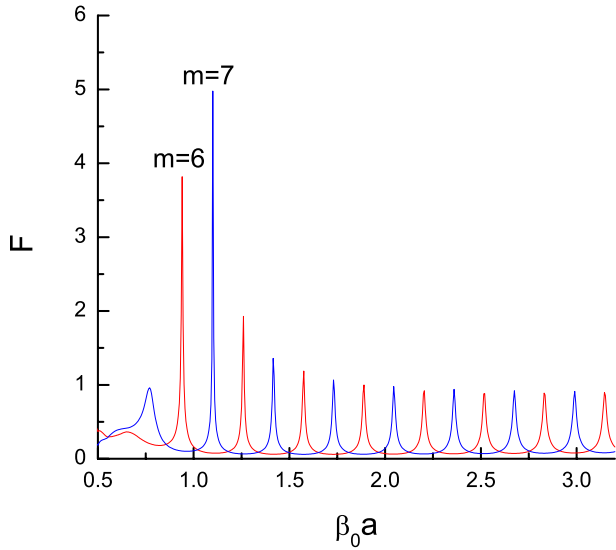


FIG. 5. (Color online) The response function plotted versus the dimensionless propagation constant for $\epsilon_1=1$, $\epsilon_2=6$, and $L/a=20$. The red and blue lines display the even and odd modes, respectively.

the same set of resonance curves can be featured by the sections $\bar{L}=\text{constant}$. A representative cross section from this family corresponding to the white horizontal lines in Figs. 3(a) and 3(b) is shown in Fig. 5. Such a set of resonances can be well described by the formula

$$\beta_0 L = m\alpha(L) - \psi(L) \quad (30)$$

with the parameters $\alpha(L)$ and $\psi(L)$ which are plotted in Figs. 6 and 7, respectively. The resonances of maximum intensity fall into the range of β_0 around the value $\beta_0=1$ where the phase $\phi(\beta_0)$ is close to zero (see Fig. 4). As it is seen from Figs. 3(a) and 3(b), the resonances of all orders have

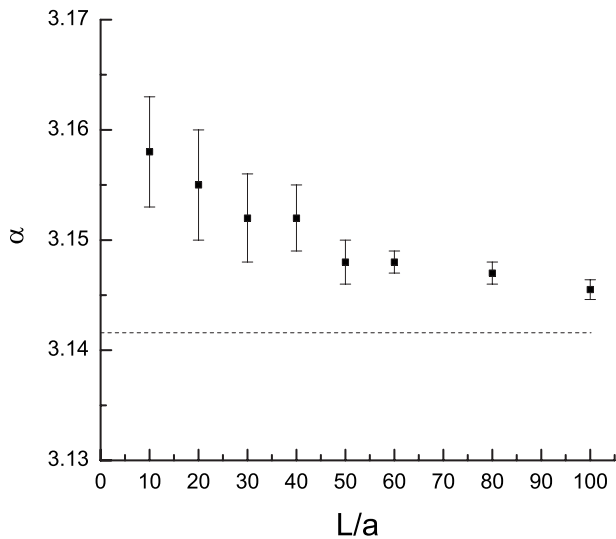


FIG. 6. The parameter α entering into Eq. (30) as a function of the dimensionless nanowire length. The horizontal dash line indicates the value of π . The error bars originate from the linear fitting of Eq. (30).

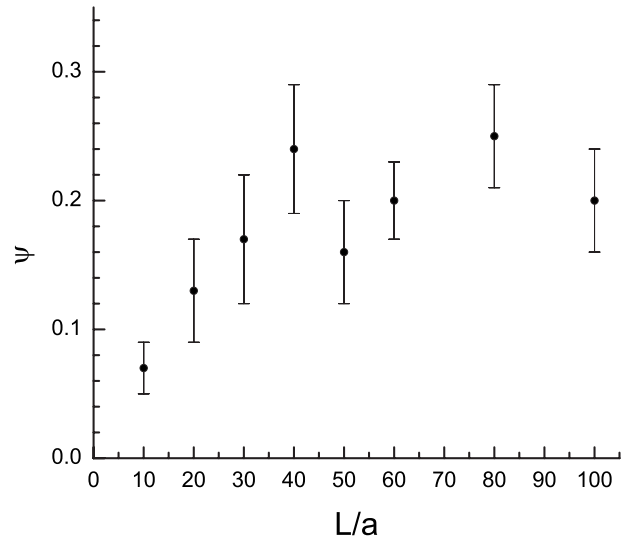


FIG. 7. The parameter ψ entering into Eq. (30) as a function of the dimensionless nanowire length. The error bars originate from the linear fitting of Eq. (30).

maximum intensity in this interval. The quality factor of the most intensive Fabry-Pérot resonance shown in Fig. 5 ($m=7$) is estimated to be $Q=240$. The spatial distributions of the E_z field component corresponding to the two Fabry-Pérot peaks indicated in Fig. 5 are shown in Fig. 8. It is clearly seen that the order of the resonance is equal to the number of half periods fitted along the nanowire length.

For the purpose of comparison with experimental results it is sometimes more convenient to have the positions of resonances in terms of the wavelength. Such plots can be obtained with the use of the dispersion relation $\omega=\omega(\beta_0)$ represented in Fig. 2. They are shown in Figs. 9(a) and 9(b) for even and odd modes, respectively.

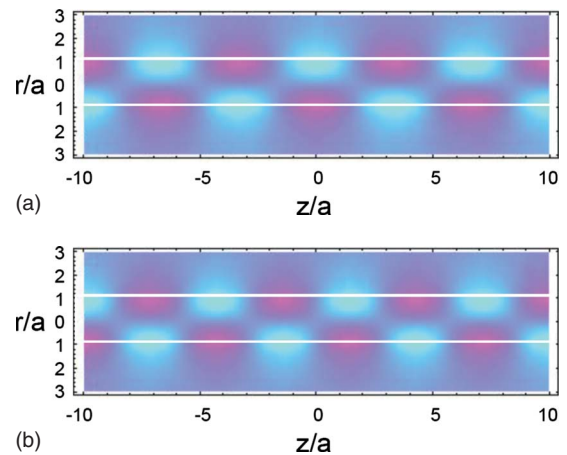


FIG. 8. (Color online) The spatial distribution of the E_z field component in the neglect of corrections at the nanowire ends for $\epsilon_1=1$, $\epsilon_2=6$ and $L/a=20$: (a) $m=6$; (b) $m=7$. The white lines indicate the cross section of the nanowire cylindrical surface. The blue and red regions correspond to positive and negative values of either real part (for an even mode) or imaginary part (for an odd mode) of the functions $S_{0,11}=S_{0,33}$ [Eq. (29)], respectively.

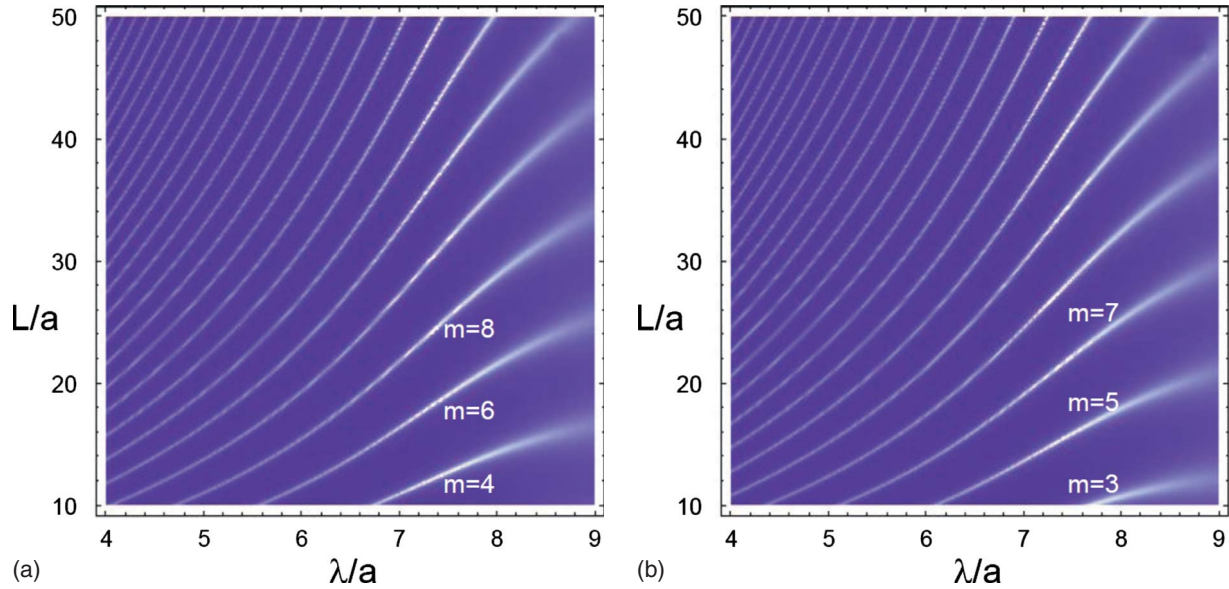


FIG. 9. (Color online) The response function plotted versus the dimensionless wavelength and NW length for $\epsilon_1=1$ and $\epsilon_2=6$: (a) even modes; (b) odd modes. The orders of the first three resonances in this range are indicated.

Let us note that both Eqs. (27) and (30) contain the non-negligible phases ϕ and ψ and in this sense they are not reduced to the formula for Fabry-Pérot resonator between two dielectric boundaries. However if one is interested in the difference between the positions of adjacent resonances those equations approximate the classical result since $\alpha(L) \approx \pi$.

The numerical results obtained here are represented in dimensionless quantities. To get absolute values of the parameters one needs to specify one of them. Let us assume, as an example, that the NW radius is equal to 100 nm. Then the above consideration is valid in the wavelength region $\lambda > 370$ nm and for nanowires much longer than $0.2 \mu\text{m}$ that is typical for experimental conditions.

IV. CONCLUSION

In conclusion, we have developed the rigorous theory which determines Fabry-Pérot modes of a nanowire. They are defined as nontrivial solutions of the integral Eq. (9) which is valid for an arbitrary nanowire length, diameter and electromagnetic field wavelength. It can be reduced to a set of linear algebraic equations in the limit of elongated nanowire when its length exceeds considerably its diameter. The results obtained for elongated nanowires which support a single waveguide mode have revealed that the condition for the nanowire Fabry-Pérot-like modes to occur can be described by the formula for classical resonator if to introduce an effective phase shift on reflection from its facets. The latter quantity can be obtained from the numerical calculations of the nanowire response function. It depends on the waveguide mode propagation constant (or on its wavelength) although the dielectric functions of both the nanowire material and surrounding medium have been assumed to be dispersionless.

In the above consideration we have implied that the propagation constants of the waveguide modes are real. The developed approach will be still valid if the dielectric function ϵ_2 , and hence the propagation constants, have an imaginary part. One can expect that Eq. (27) will be fulfilled approximately for $\text{Re}(\beta_0)$ provided that the attenuation of the waveguide mode amplitude at the NW length is negligible. In the case of a metal nanowire all modes have complex propagation constants.³⁵ One can distinguish between strongly decaying bulk modes and surface-plasmon polariton modes which propagate over relatively long distances. The approach developed above can be equally applied to metal nanowires if instead of the waveguide modes one will consider surface modes whose propagation length is comparable with or larger than the nanowire length.³⁶ There are only two surface modes, TM_0 and HE_1 , which have no cutoff. The higher order surface modes, HE_n with $n > 1$, convert to radiating ones below cutoff. The HE_1 mode propagation constant equals approximately the wave number in the surrounding medium. This mode does not contribute to the Fabry-Pérot modes due to a low effective refractive index contrast. Therefore only the TM_0 mode dictates the resonance conditions in a metal nanowire Fabry-Pérot cavity.

ACKNOWLEDGMENT

The author would like to thank Morten Willatzen for reading the paper and valuable comments.

APPENDIX: EXPLICIT FORM OF THE MATRICES \hat{M}_n AND \hat{N}_n

The matrix \hat{M}_n has the following form:

$$\hat{M}_n(\beta) = \begin{pmatrix} (\beta n/q_2^2 a) J_n(q_2 a) & -(i\omega/c q_2) J'_n(q_2 a) & -(\beta n/q_1^2 a) H_n^{(1)}(q_1 a) & (i\omega/c q_1) H_n^{(1)'}(q_1 a) \\ J_n(q_2 a) & 0 & -H_n^{(1)}(q_1 a) & 0 \\ (ik_2^2 c/\omega q_2) J'_n(q_2 a) & (\beta n/q_2^2 a) J_n(q_2 a) & -(ik_1^2 c/\omega q_1) H_n^{(1)'}(q_1 a) & -(\beta n/q_1^2 a) H_n^{(1)}(q_1 a) \\ 0 & J_n(q_2 a) & 0 & -H_n^{(1)}(q_1 a) \end{pmatrix}. \quad (\text{A1})$$

The matrix \hat{N}_n can be found using the results of Ref. 29. Its matrix elements are given by

$$[\hat{N}_n(\beta, \beta')]_{11} = \frac{\pi^2}{\omega} \left\{ - \left[ik_2^2 \pi_{2,-1}^{\epsilon,1}(\beta, \beta') + \frac{\omega}{c} \beta \pi_{2,-1}^{m,1}(\beta, \beta') \right] H_{n-1}^{(1)}(q_2 a) + \left[ik_2^2 \pi_{2,1}^{\epsilon,1}(\beta, \beta') - \frac{\omega}{c} \beta \pi_{2,1}^{m,1}(\beta, \beta') \right] H_{n+1}^{(1)}(q_2 a) + i \frac{nq_2}{a} [\pi_{2,-1}^{\epsilon,1}(\beta, \beta') - \pi_{2,1}^{\epsilon,1}(\beta, \beta')] H_n^{(1)}(q_2 a) \right\}, \quad (\text{A2})$$

$$[\hat{N}_n(\beta, \beta')]_{12} = \frac{\pi^2}{\omega} \left\{ - \left[ik_2^2 \pi_{2,-1}^{\epsilon,2}(\beta, \beta') + \frac{\omega}{c} \beta \pi_{2,-1}^{m,2}(\beta, \beta') \right] H_{n-1}^{(1)}(q_2 a) + \left[ik_2^2 \pi_{2,1}^{\epsilon,2}(\beta, \beta') - \frac{\omega}{c} \beta \pi_{2,1}^{m,2}(\beta, \beta') \right] H_{n+1}^{(1)}(q_2 a) + i \frac{nq_2}{a} [\pi_{2,-1}^{\epsilon,2}(\beta, \beta') - \pi_{2,1}^{\epsilon,2}(\beta, \beta')] H_n^{(1)}(q_2 a) \right\}, \quad (\text{A3})$$

$$[\hat{N}_n(\beta, \beta')]_{13} = \frac{\pi^2}{\omega} \left\{ \left[ik_1^2 \pi_{1,-1}^{\epsilon,3}(\beta, \beta') + \frac{\omega}{c} \beta \pi_{1,-1}^{m,3}(\beta, \beta') \right] J_{n-1}(q_1 a) - \left[ik_1^2 \pi_{1,1}^{\epsilon,3}(\beta, \beta') - \frac{\omega}{c} \beta \pi_{1,1}^{m,3}(\beta, \beta') \right] J_{n+1}(q_1 a) - i \frac{nq_1}{a} [\pi_{1,-1}^{\epsilon,3}(\beta, \beta') - \pi_{1,1}^{\epsilon,3}(\beta, \beta')] J_n(q_1 a) \right\}, \quad (\text{A4})$$

$$[\hat{N}_n(\beta, \beta')]_{14} = \frac{\pi^2}{\omega} \left\{ \left[ik_1^2 \pi_{1,-1}^{\epsilon,4}(\beta, \beta') + \frac{\omega}{c} \beta \pi_{1,-1}^{m,4}(\beta, \beta') \right] J_{n-1}(q_1 a) - \left[ik_1^2 \pi_{1,1}^{\epsilon,4}(\beta, \beta') - \frac{\omega}{c} \beta \pi_{1,1}^{m,4}(\beta, \beta') \right] J_{n+1}(q_1 a) - i \frac{nq_1}{a} [\pi_{1,-1}^{\epsilon,4}(\beta, \beta') - \pi_{1,1}^{\epsilon,4}(\beta, \beta')] J_n(q_1 a) \right\}, \quad (\text{A5})$$

$$[\hat{N}_n(\beta, \beta')]_{21} = -\frac{\pi^2}{\omega} q_2 \left\{ i\beta [\pi_{2,-1}^{\epsilon,1}(\beta, \beta') - \pi_{2,1}^{\epsilon,1}(\beta, \beta')] + \frac{\omega}{c} [\pi_{2,-1}^{m,1}(\beta, \beta') + \pi_{2,1}^{m,1}(\beta, \beta')] \right\} H_n^{(1)}(q_2 a), \quad (\text{A6})$$

$$[\hat{N}_n(\beta, \beta')]_{22} = -\frac{\pi^2}{\omega} q_2 \left\{ i\beta [\pi_{2,-1}^{\epsilon,2}(\beta, \beta') - \pi_{2,1}^{\epsilon,2}(\beta, \beta')] + \frac{\omega}{c} [\pi_{2,-1}^{m,2}(\beta, \beta') + \pi_{2,1}^{m,2}(\beta, \beta')] \right\} H_n^{(1)}(q_2 a), \quad (\text{A7})$$

$$[\hat{N}_n(\beta, \beta')]_{23} = \frac{\pi^2}{\omega} q_1 \left\{ i\beta [\pi_{1,-1}^{\epsilon,3}(\beta, \beta') - \pi_{1,1}^{\epsilon,3}(\beta, \beta')] + \frac{\omega}{c} [\pi_{1,-1}^{m,3}(\beta, \beta') + \pi_{1,1}^{m,3}(\beta, \beta')] \right\} J_n(q_1 a), \quad (\text{A8})$$

$$[\hat{N}_n(\beta, \beta')]_{24} = \frac{\pi^2}{\omega} q_1 \left\{ i\beta [\pi_{1,-1}^{\epsilon,4}(\beta, \beta') - \pi_{1,1}^{\epsilon,4}(\beta, \beta')] + \frac{\omega}{c} [\pi_{1,-1}^{m,4}(\beta, \beta') + \pi_{1,1}^{m,4}(\beta, \beta')] \right\} J_n(q_1 a), \quad (\text{A9})$$

$$[\hat{N}_n(\beta, \beta')]_{31} = \frac{\pi^2}{\omega} \left\{ - \left[ik_2^2 \pi_{2,-1}^{m,1}(\beta, \beta') - \frac{\omega}{c} \beta \epsilon_2 \pi_{2,-1}^{\epsilon,1}(\beta, \beta') \right] H_{n-1}^{(1)}(q_2 a) + \left[ik_2^2 \pi_{2,1}^{m,1}(\beta, \beta') + \frac{\omega}{c} \beta \epsilon_2 \pi_{2,1}^{\epsilon,1}(\beta, \beta') \right] H_{n+1}^{(1)}(q_2 a) + i \frac{nq_2}{a} [\pi_{2,-1}^{m,1}(\beta, \beta') - \pi_{2,1}^{m,1}(\beta, \beta')] H_n^{(1)}(q_2 a) \right\}, \quad (\text{A10})$$

$$[\hat{N}_n(\beta, \beta')]_{32} = \frac{\pi^2}{\omega} \left\{ - \left[ik_2^2 \pi_{2,-1}^{m,2}(\beta, \beta') - \frac{\omega}{c} \beta \epsilon_2 \pi_{2,-1}^{\epsilon,2}(\beta, \beta') \right] H_{n-1}^{(1)}(q_2 a) + \left[ik_2^2 \pi_{2,1}^{m,2}(\beta, \beta') + \frac{\omega}{c} \beta \epsilon_2 \pi_{2,1}^{\epsilon,2}(\beta, \beta') \right] H_{n+1}^{(1)}(q_2 a) + i \frac{nq_2}{a} [\pi_{2,-1}^{m,2}(\beta, \beta') - \pi_{2,1}^{m,2}(\beta, \beta')] H_n^{(1)}(q_2 a) \right\}, \quad (\text{A11})$$

$$[\hat{N}_n(\beta, \beta')]_{33} = \frac{\pi^2}{\omega} \left\{ \left[ik_1^2 \pi_{1,-1}^{m,3}(\beta, \beta') - \frac{\omega}{c} \beta \epsilon_1 \pi_{1,-1}^{e,3}(\beta, \beta') \right] J_{n-1}(q_1 a) - \left[ik_1^2 \pi_{1,1}^{m,3}(\beta, \beta') + \frac{\omega}{c} \beta \epsilon_1 \pi_{1,1}^{e,3}(\beta, \beta') \right] J_{n+1}(q_1 a) - i \frac{nq_1}{a} [\pi_{1,-1}^{m,3}(\beta, \beta') - \pi_{1,1}^{m,3}(\beta, \beta')] J_n(q_1 a) \right\}, \quad (\text{A12})$$

$$[\hat{N}_n(\beta, \beta')]_{34} = \frac{\pi^2}{\omega} \left\{ \left[ik_1^2 \pi_{1,-1}^{m,4}(\beta, \beta') - \frac{\omega}{c} \beta \epsilon_1 \pi_{1,-1}^{e,4}(\beta, \beta') \right] J_{n-1}(q_1 a) - \left[ik_1^2 \pi_{1,1}^{m,4}(\beta, \beta') + \frac{\omega}{c} \beta \epsilon_1 \pi_{1,1}^{e,4}(\beta, \beta') \right] J_{n+1}(q_1 a) - i \frac{nq_1}{a} [\pi_{1,-1}^{m,4}(\beta, \beta') - \pi_{1,1}^{m,4}(\beta, \beta')] J_n(q_1 a) \right\}, \quad (\text{A13})$$

$$[\hat{N}_n(\beta, \beta')]_{41} = -\frac{\pi^2}{\omega} \left\{ i\beta [\pi_{2,-1}^{m,1}(\beta, \beta') - \pi_{2,1}^{m,1}(\beta, \beta')] - \frac{\omega}{c} \epsilon_2 [\pi_{2,-1}^{e,1}(\beta, \beta') + \pi_{2,1}^{e,1}(\beta, \beta')] \right\} H_n^{(1)}(q_2 a), \quad (\text{A14})$$

$$[\hat{N}_n(\beta, \beta')]_{42} = -\frac{\pi^2}{\omega} q_2 \left\{ i\beta [\pi_{2,-1}^{m,2}(\beta, \beta') - \pi_{2,1}^{m,2}(\beta, \beta')] - \frac{\omega}{c} \epsilon_2 [\pi_{2,-1}^{e,2}(\beta, \beta') + \pi_{2,1}^{e,2}(\beta, \beta')] \right\} H_n^{(1)}(q_2 a), \quad (\text{A15})$$

$$[\hat{N}_n(\beta, \beta')]_{43} = \frac{\pi^2}{\omega} q_1 \left\{ i\beta [\pi_{1,-1}^{m,3}(\beta, \beta') - \pi_{1,1}^{m,3}(\beta, \beta')] - \frac{\omega}{c} \epsilon_1 [\pi_{1,-1}^{e,3}(\beta, \beta') + \pi_{1,1}^{e,3}(\beta, \beta')] \right\} J_n(q_1 a), \quad (\text{A16})$$

$$[\hat{N}_n(\beta, \beta')]_{44} = \frac{\pi^2}{\omega} q_1 \left\{ i\beta [\pi_{1,-1}^{m,4}(\beta, \beta') - \pi_{1,1}^{m,4}(\beta, \beta')] - \frac{\omega}{c} \epsilon_1 [\pi_{1,-1}^{e,4}(\beta, \beta') + \pi_{1,1}^{e,4}(\beta, \beta')] \right\} J_n(q_1 a). \quad (\text{A17})$$

Here we have introduced the following functions:

$$\pi_{j,\mu}^{\sigma,k}(\beta, \beta') = \frac{1}{\tau_j^\sigma} \frac{a}{\beta^2 - \beta'^2} C_{j,\mu}^{\sigma,k}(\beta') D_{j,\mu}(\beta, \beta'), \quad (\text{A18})$$

where $\sigma = e, m$, $k = 1, 2, 3, 4$, $j = 1, 2$, $\mu = \pm 1$, $\tau_j^e = \epsilon_j$, $\tau_j^m = 1$, and

$$C_{2,1}^{e,1}(\beta) = -C_{2,-1}^{e,1}(\beta) = i \frac{c^2 k_2^2}{4\pi\omega q_2}, \quad (\text{A19})$$

$$C_{2,1}^{e,2}(\beta) = C_{2,-1}^{e,2}(\beta) = -\frac{c\beta}{4\pi q_2}, \quad (\text{A20})$$

$$C_{1,1}^{e,3}(\beta) = -C_{1,-1}^{e,3}(\beta) = -i \frac{c^2 k_1^2}{4\pi\omega q_1}, \quad (\text{A21})$$

$$C_{1,1}^{e,4}(\beta) = C_{1,-1}^{e,4}(\beta) = \frac{c\beta}{4\pi q_1}, \quad (\text{A22})$$

$$C_{2,1}^{m,1}(\beta) = C_{2,-1}^{m,1}(\beta) = \frac{c\beta}{4\pi q_2}, \quad (\text{A23})$$

$$C_{2,1}^{m,2}(\beta) = -C_{2,-1}^{m,2}(\beta) = i \frac{\omega}{4\pi q_2}, \quad (\text{A24})$$

$$C_{1,1}^{m,3}(\beta) = C_{1,-1}^{m,3}(\beta) = -\frac{c\beta}{4\pi q_1}, \quad (\text{A25})$$

$$C_{1,1}^{m,4}(\beta) = -C_{1,-1}^{m,4}(\beta) = -i \frac{\omega}{4\pi q_1}, \quad (\text{A26})$$

$$D_{j,\mu}(\beta, \beta') = q'_j Z_{n+\mu}(q_j a) Z_{n+\mu-1}(q'_j a) - q_j Z_{n+\mu-1}(q_j a) Z_{n+\mu}(q'_j a) \quad (\text{A27})$$

with $q'_j = \sqrt{k_j^2 - \beta'^2}$ and

$$Z_m(q_j a) = \begin{cases} H_m^{(1)}(q_1 a) & \text{if } j = 1 \\ J_m(q_2 a) & \text{if } j = 2 \end{cases}. \quad (\text{A28})$$

When calculating the matrix elements of $\hat{N}_n(\beta, \beta')$ at $\beta' \rightarrow \beta$ one should use the limit

$$\lim_{\beta' \rightarrow \beta} \pi_{j,\mu}^{\sigma,k}(\beta, \beta') = -\frac{a^2}{2\tau_j^\sigma} C_{j,\mu}^{\sigma,k}(\beta) D_{j,\mu}^0(\beta) \quad (\text{A29})$$

with

$$D_{j,\mu}^0(\beta) = [Z_{n+\mu}(q_j a)]^2 - Z_{n+\mu-1}(q_j a) Z_{n+\mu+1}(q_j a). \quad (\text{A30})$$

- *On leave from A.M. Prokhorov General Physics Institute, Russian Academy of Sciences, 119991 Moscow, Russia; bordo@mci.sdu.dk
- ¹Y. Li, F. Qian, J. Xiang, and C. M. Lieber, *Mater. Today* **9**, 18 (2006).
 - ²P. J. Pauzauskis and P. Yang, *Mater. Today* **9**, 36 (2006).
 - ³F. Balzer, V. G. Bordo, R. Neuendorf, K. Al-Shamery, A. C. Simonsen, and H.-G. Rubahn, *IEEE Trans. Nanotechnol.* **3**, 67 (2004).
 - ⁴W. L. Barnes, A. Dereux, and T. W. Ebbesen, *Nature (London)* **424**, 824 (2003).
 - ⁵M. Pelton, J. Aizpurua, and G. Bryant, *Laser Photonics Rev.* **2**, 136 (2008).
 - ⁶T. H. Taminiou, R. J. Moerland, F. B. Segerink, L. Kuipers, and N. F. van Hulst, *Nano Lett.* **7**, 28 (2007).
 - ⁷A. Alù and N. Engheta, *Nat. Photonics* **2**, 307 (2008).
 - ⁸I. Friedler, C. Sauvan, J. P. Hugonin, P. Lalanne, J. Claudon, and J. M. Gérard, *Opt. Express* **17**, 2095 (2009).
 - ⁹B. Hua, J. Motohisa, Y. Ding, S. Hara, and T. Fukui, *Appl. Phys. Lett.* **91**, 131112 (2007).
 - ¹⁰Y. Ding, J. Motohisa, B. Hua, S. Hara, and T. Fukui, *Nano Lett.* **7**, 3598 (2007).
 - ¹¹S. Rühle, L. K. van Vugt, H.-Y. Li, N. A. Keizer, L. Kuipers, and D. Vanmaekelbergh, *Nano Lett.* **8**, 119 (2008).
 - ¹²B. Hua, J. Motohisa, S. Hara and T. Fukui, *Phys. Status Solidi C* **5**, 2722 (2008).
 - ¹³H. Ditlbacher, A. Hohenau, D. Wagner, U. Kreibig, M. Rogers, F. Hofer, F. R. Aussenegg, and J. R. Krenn, *Phys. Rev. Lett.* **95**, 257403 (2005).
 - ¹⁴M. Allione, V. V. Temnov, Y. Fedutik, U. Woggon, and M. V. Artemyev, *Nano Lett.* **8**, 31 (2008).
 - ¹⁵X. Duan, Y. Huang, R. Agarwal, and C. M. Lieber, *Nature (London)* **421**, 241 (2003).
 - ¹⁶J. C. Johnson, H. Yan, P. Yang, and R. J. Saykally, *J. Phys. Chem. B* **107**, 8816 (2003).
 - ¹⁷M. A. Zimmier, J. Bao, F. Capasso, S. Müller, and C. Ronning, *Appl. Phys. Lett.* **93**, 051101 (2008).
 - ¹⁸D. J. Bergman and M. I. Stockman, *Phys. Rev. Lett.* **90**, 027402 (2003).
 - ¹⁹L. K. van Vugt, B. Zhang, B. Piccone, A. A. Spector, and R. Agarwal, *Nano Lett.* **9**, 1684 (2009).
 - ²⁰M. Born and E. Wolf, *Principles of Optics: Electromagnetic Theory of Propagation, Interference and Diffraction of Light* (Cambridge University Press, Cambridge, 1997).
 - ²¹A. N. Chin, S. Vaddiraju, A. V. Maslov, C. Z. Ning, M. K. Sunkara, and M. Meyyappan, *Appl. Phys. Lett.* **88**, 163115 (2006).
 - ²²L. K. van Vugt, S. Rühle, and D. Vanmaekelbergh, *Nano Lett.* **6**, 2707 (2006).
 - ²³K. Takazawa, *J. Phys. Chem. C* **111**, 8671 (2007).
 - ²⁴L. Yang, J. Motohisa, T. Fukui, L. X. Jia, L. Zhang, M. M. Geng, P. Chen, and Y. L. Liu, *Opt. Express* **17**, 9337 (2009).
 - ²⁵T. Søndergaard, J. Beermann, A. Boltasseva, and S. I. Bozhevolnyi, *Phys. Rev. B* **77**, 115420 (2008).
 - ²⁶E. S. Barnard, J. S. White, A. Chandran, and M. L. Brongersma, *Opt. Express* **16**, 16529 (2008).
 - ²⁷J. A. Stratton, *Electromagnetic Theory* (McGraw-Hill, New York, 1941).
 - ²⁸S. A. Schelkunoff, *Phys. Rev.* **56**, 308 (1939).
 - ²⁹V. G. Bordo, *Phys. Rev. B* **78**, 085318 (2008); **79**, 039901(E) (2009).
 - ³⁰This statement is not valid for metal nanowires for which the frequency dispersion of ϵ_2 is essential.
 - ³¹W. H. Press, S. A. Teukolsky, W. T. Vetterling, and B. P. Flannery, *Numerical Recipes. The Art of Scientific Computing* (Cambridge University Press, Cambridge, 2007).
 - ³²A. W. Snyder and J. D. Love, *Optical Waveguide Theory* (Chapman and Hall, London, 1983).
 - ³³In Ref. 29, an attempt was made to introduce the reflection coefficient in terms of the coordinate-independent quantity.
 - ³⁴A. V. Maslov and C. Z. Ning, *Appl. Phys. Lett.* **83**, 1237 (2003).
 - ³⁵L. Novotny and C. Hafner, *Phys. Rev. E* **50**, 4094 (1994).
 - ³⁶K. Leosson, T. Nikolajsen, A. Boltasseva, and S. I. Bozhevolnyi, *Opt. Express* **14**, 314 (2006).